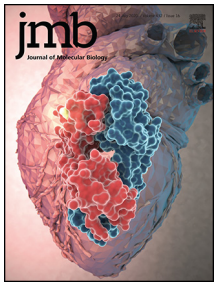

Early But Not Delayed Optogenetic RAF Activation Promotes Astrocytogenesis in Mouse Neural Progenitors

Yixun Su[1,†], Xiaomin Huang[1,†], Zhangsen Huang[1], Taida Huang[1], Tao Li[2], Huaxun Fan[3], Kai Zhang[3] and Chenju Yi[1]

*1 - **The Seventh Affiliated Hospital of Sun Yat-sen University,** Shenzhen 518107, China*
*2 - **Department of Histology and Embryology,** Chongqing Key Laboratory of Neurobiology, Army Medical University (Third Military Medical University), Chongqing 400038, China*
*3 - **Department of Biochemistry,** School of Molecular and Cellular Biology, University of Illinois at Urbana-Champaign, Urbana, IL 61801, USA*

***Correspondence to Kai Zhang and Chenju Yi:** kaizkaiz@illinois.edu, yichj@mail.sysu.edu.cn*
https://doi.org/10.1016/j.jmb.2020.06.020
Edited by Dr M Yaniv

Abstract

The RAS/RAF/MEK/ERK pathway promotes gliogenesis but the kinetic role of RAF1, a key RAF kinase, in the induction of astrocytogenesis remains to be elucidated. To address this challenge, we determine the temporal functional outcome of RAF1 during mouse neural progenitor cell differentiation using an optogenetic RAF1 system (OptoRAF1). OptoRAF1 allows for reversible activation of the RAF/MEK/ERK pathway *via* plasma membrane recruitment of RAF1 based on blue light-sensitive protein dimerizer CRY2/CIB1. We found that early light-induced OptoRAF1 activation in neural progenitor cells promotes cell proliferation and increased expression of glial markers and glia-enriched genes. However, delayed OptoRAF1 activation in differentiated neural progenitor had little effect on glia marker expression, suggesting that RAF1 is required to promote astrocytogenesis only within a short time window. In addition, activation of OptoRAF1 did not have a significant effect on neurogenesis, but was able to promote neuronal neurite growth.

Introduction

Astrocytes are one of the most abundant cell types in the mammalian brain and play crucial roles in brain development, function and phathologies. As neural progenitors lose their neurogenic potential during late stages of gestation, they transform into astrocyte precursors [1,2], which then migrate and proliferate to populate the brain as they mature.

The RAS/RAF/MEK/ERK pathway, which controls expression of genes involved in cell proliferation, differentiation, and cell death, is an essential part of a complex molecular network that regulates astrocytogenesis [1,3]. Exact regulating mechanism of neural progenitor differentiation, however, remains unclear. On the one hand, *in vitro* studies have shown that RAF activation promotes neural progenitor proliferation but favors astrocytogenesis over neurogenesis in high-density cell cultures [4]. In this scenario, reduction of the overall percentage of neuron population could arise from favored cell proliferation in gliogenic progenitors and immature astrocytes [5]. Indeed, mutant mice with RAF gain-of function do not display altered neuron numbers in the brain but possess an overproduction of astrocytes [6,7]. On the other hand, the RAF downstream pathway is necessary for neurogenesis and neurite outgrowth [4,8,9], as evidenced by the fact that the MEK-C/EBP axis promotes cortical neurogenesis [10] instead of gliogenesis [11]. Further downstream of MEK, both ERK1/2 have also been implicated in the maintenance of neural progenitor states [12]. These studies indicate that the regulation of RAF and its downstream pathways have complex implications for neural progenitor differentiation. Of particular interests is whether the temporal kinetics

of the RAF/MEK/ERK signaling leads to a diverse functional outcome during neural progenitor differentiation, as a study points out that RAF activation only promotes proliferation of astrocyte precursors, but has little effect on the proliferative potential of mature astrocytes [5].

Most of the current gain-of-function studies conducted with the RAS/RAF/MEK/ERK pathway rely on the use of growth factor or overexpression of constitutively active mutants [13]. Unfortunately, growth factors may activate pathways apart from the RAS/RAF/MEK/ERK pathway, while overexpression models could induce a negative feedback response that negates the phenotype particularly in chronic mice model. For instance, knock-in of constitutive active RAF mutants in mice does not result in the activation of MEK or ERK [6,7].

The emerging optogenetic techniques could be an alternative strategy to address some of these challenges [14]. Recent advances in optogenetics have enabled spatial and temporal regulation of endogenous protein, protein–protein interaction, and intracellular signaling pathways in live cells and multicellular organisms. [15–22]. We have previously developed an optogenetic tool that allows for reversible activation of the RAF/MEK/ERK pathway (OptoRAF1) in mammalian cells and *Xenopus laevis* [15,23–25]. Here, we apply this tool in primary mouse neural progenitor cells to gain insights into the time-dependent signaling outcome during neural progenitor differentiation. We found that early OptoRAF1 activation in neural progenitor promotes cell proliferation and increased expression of glial markers and glia-enriched genes. Delayed OptoRAF1 activation, however, failed to induce astrocytogenesis. These results pin down a short time window (less than 2 days) during which RAF1 activation promotes astrocytogenesis. In addition, activation of OptoRAF1 did not have a significant effect on neurogenesis, but it promotes neuronal neurite growth.

Results

Optogenetic activation of RAF signaling pathway in neural progenitors

We first confirmed that OptoRAF1 system successfully activates the ERK signaling pathway in the primary mouse neural progenitor cells. The OptoRAF1 system consists of two fusion proteins: human RAF1 protein fused to the CRY2 protein (CRY2–RAF1), and the CIBN (N terminus of CIB1) to the plasma membrane anchoring peptide CAAX (CIBN-CAAX) [23–25]. Briefly, in cells co-expressing these two proteins, blue light exposure induces the oligomerization of CRY2–RAF1 and recruits it to the plasma membrane by its interaction with anchored CIBN-CAAX. At the plasma membrane, it interacts with RAS protein, resulting in the activation of RAF and associated downstream pathways (Figure 1(a)). For long-term illumination, we constructed an LED light box which allows for a programmable light-on/off cycle. Based on previous experiments, the light cycle was set to 20-min-on, 40-min-off mode to achieve optimal RAF signaling output (Figure 1(c)) [23,26]. To validate the activation of RAF downstream pathway after light illumination, we subjected the OptoRAF1-infected neural progenitors to light for 15 min, then analyzed the activation of ERK1/2 by flow cytometry, confirming that the light illumination led to increased activation of the RAF–ERK pathway (Figure 1(b)).

Early OptoRAF1 activation promotes astrocytogenesis

To determine how timed activation of the RAF/MEK/ERK pathway regulates neural progenitor differentiation, we first activated OptoRAF1 during an early course of neural progenitor differentiation. We introduced the OptoRAF1 system into E15 neural progenitors 4 days *in vitro* (DIV4), withdrew growth factor treatment the next day to initiate cell differentiation, and started the light illumination cycles, each of which contains a pulsatile 20-min-on, 40-min-off period. The cells were collected 4 days after growth factor withdrawal for analysis (Figure 1(c)). Apart from the treatment group (Light OptoRAF1), three control groups were set up: cells infected with GFP and maintained in the dark (Dark GFP), cells infected with OptoRAF1 and maintained in the dark (Dark OptoRAF1), and cells infected with GFP and illuminated (Light GFP). Immunostaining of the astrocyte marker GFAP showed that light-induced OptoRAF1 activation in neural progenitors yielded a higher proportion of astrocytes (Figure 1(d) and (f)). Illumination or OptoRAF1 infection alone did not have a significant effect on GFAP + cell percentage.

DAPI staining showed that OptoRAF1 activation also resulted in higher total cell counts (Figure S1B), likely due to increased cell proliferation or preservation of an immature glia state. To confirm that OptoRAF1 activation promotes proliferation, we conducted BrdU incorporation assays. Results demonstrated that OptoRAF1 activation resulted in an increased number of BrdU + cells, suggesting that OptoRAF1 activation increases proliferation (Figure 1(e) and (g)). On the other hand, the radial glia and immature glia marker Brain lipid-binding protein (BLBP/FABP7) could be found in all cells observed (Figure 1(e)).

Early OptoRAF1 activation promotes astrocyte maturation

We observed that light-induced RAF1 activation during early cell differentiation resulted in an increased number of processes in GFAP + cells, while those in the

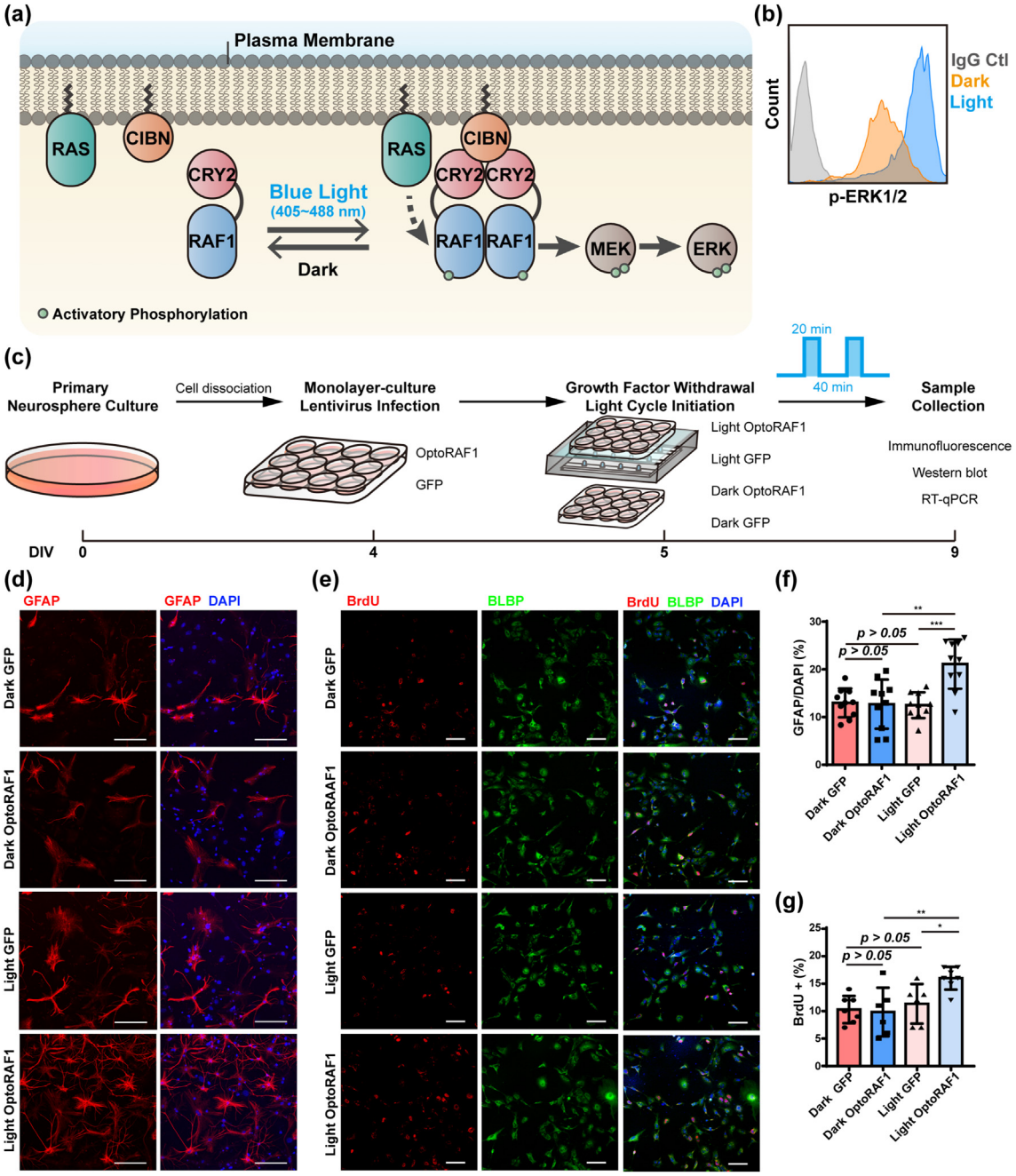

Figure 1. Light-induced OptoRAF1 activation promoted astrocytogenesis and cell proliferation. (a) Illustration of the OptoRAF1 system. Upon blue light (405 ~ 488 nm) illumination, CRY2–RAF1 dimerizes and binds to membrane-anchored CAAX-CIBN. This allows RAF1 to be in the proximity of RAS proteins, which promotes RAF1 activation and the initiation of downstream pathways. (b) Flow cytometry confirmed that OptoRAF1-infected neural progenitors display increased ERK1/2 activation when exposed to blue light. (c) OptoRAF1 infected neural progenitors were allowed to differentiate and were illuminated simultaneously for 4 days before sample collection. (d) Immunostaining of GFAP. The scale bar represents 50 μm. (e) Immunostaining of BLBP and BrdU after BrdU incorporation. The scale bar represents 50 μm. (f) Quantification of GFAP+ cell percentage. (g) Quantification of BrdU+ cell percentage. *** $p < 0.005$, ** $p < 0.01$, * $p < 0.05$, (N = 3, n ≥ 3).

control groups display a more pronounced immature astrocyte phenotype (Figure S1A). We further examined whether early RAF activation promotes astrocyte maturation. We analyzed the expression of several mature astrocyte markers that are crucial for astrocyte functions, by first examining the expression of

connexin43 (Cx43), an astrocyte-enriched channel-forming protein, which is crucial for the function of astrocytic network. Results showed that light-induced OptoRAF1 activation led to an increased Cx43 puncta number per cell, which was correlated with an increased number of astrocytes (Figures 2(a) and S1C). In addition, the number of Cx43 puncta per astrocyte was also increased in the Light-OptoRAF1 group (Figure 2(b)). Similarly, glucose transporter 1 (GLUT1) signal intensity and GLUT1 + cell percentage, as shown by immunostaining, were significantly increased in the OptoRAF1 activation group (Figure 2(c)–(d), Figure S1D). In addition, while the percentage of Aldehyde Dehydrogenase 1 Family Member L1 (ALDH1L1)+ cells was unchanged, the signal intensity of ALDH1L1 was slightly increased by OptoRAF1 activation (Figures 2(e)–(f) and S1E). The S100 calcium-binding protein B (S100beta)+ cell percentage was increased in the OptoRAF1 activation group, while the S100beta signal intensity was unaltered (Figures 2(e) and (g) and S1F).

To further confirm that OptoRAF1 activation promotes astrocytogenesis and astrocyte maturation, RT-qPCR experiment was performed on differentiated neural progenitors. Concomitant with the immunostaining results, RT-qPCR showed that OptoRAF1 activation led to increased expression of astrocyte markers *Fabp7*, *Gfap*, and *Aldh1l1*. However, expression of *Aqp4* (Aquaporin 4), another marker for astrocyte maturation, did not significantly increase in response to OptoRAF1 activation (Figure 3(a)–(d)). Furthermore, Western blotting also demonstrated increased expression of ALDH1L1 and GFAP after OptoRAF1 activation (Figure 3(e)–(g)). These data suggest that light-induced OptoRAF1 activation promotes not only astrocytogenesis but also astrocyte maturation.

Delayed OptoRAF1 activation does not promote astrocytogenesis

Next, we sought to understand if a delayed activation of OptoRAF1 could still promote astrocyte proliferation and/or maturation. Compared with the early OptoRAF1 activation scheme, the delayed activation scheme inserted two extra days to allow the isolated neural progenitors to differentiate in growth factors-deprived medium before light illumination (Figure 4(a)). Immunocytochemistry showed that delayed activation of OptoRAF1 did not significantly increase the percentage of GFAP + cells (Figure 4(b) and (c)). Nonetheless, it was still able to promote Cx43 expression in astrocytes (Figure 4(b), (d), (e)). Delayed OptoRAF1 activation was not able to promote proliferation, as shown by counting total cell numbers (Figure 4(f)), which was confirmed by the BrdU incorporation assay (Figure 5(a) and (c)). The proportion of BLBP + cells was also not significantly changed by delayed OptoRAF1 activation (Figure 5(b)).

In addition, delayed activation of OptoRAF1 did not significantly alter ALDH1L1 or GLUT1 expression (Figure S2). RT-qPCR of RNA obtained from treated neural progenitors suggested that delayed OptoRAF1 activation resulted in slight, yet not significant increase of the expression level of Gfap, Aldh1l1, and Aqp4 (Figure 6(a)–(d)). Similarly, Western blot showed that delayed OptoRAF1 activation was able to result in increased ALDH1L1 and GFAP expression, though much less than that in the early activation scheme (Figure 6(e)–(g)). Taken together, these data suggest that delayed RAF1 activation is not sufficient to promote astrocytogenesis and maturation of astrocyte in the later stage of differentiation.

Dose-dependent effect of OptoRAF1 activation on astrocytogenesis

Taking advantages of the precise temporal control of optoRAF1, we attempted to determine if astrocytogenesis depends on the total duration of RAF1 activation. To do so, we lowered the frequency of RAF1 activation by administrating a pattern of light stimulation with extended dark period (20-min-on, 120-min-off). Compared with the 20-min-on, 40-min-off illumination cycle, this new pattern maintained the duration of RAF1 activation in each on cycle but stretched the period for inactivated RAF1. The net effect is that the frequency of RAF1 activation is reduced in this 20-min-on, 120-min-off pattern, resulting in an overall lower level of RAF1 activation [23,26] (Figure S3A). Unlike the high-frequency (20-min on, 40-min off) RAF1 activation, this low-frequency RAF1 activation did not increase the level of GFAP protein measured by immunostaining. Similarly, RT-qPCR showed that the 20-min-on, 120-min-off cycle failed to promote expression of astrocyte markers (Figure S3C). Interestingly, this low-frequency RAF1 activation sufficed to promote Cx43 expression (Figure S3B). Thus, RAF1 regulates astrocytogenesis in a dose-dependent manner but the expression of different astrocyte genes may require distinct span of RAF1 activation.

Light-induced OptoRAF1 activation does not suppress neurogenesis

Considering hyperactivation of the RAS–ERK pathway has been shown to inhibit neurogenesis [27,28], we aimed to determine if Light-OptoRAF1 could promote astrocytogenesis at the expense of neurogenesis. Immunostaining of the neuron marker MAP2 suggests that OptoRAF1 activation did not significantly alter the proportion of post-differentiation neurons (Figure S4A and B). Nevertheless, we found that RAF1 activation was able to enhance neurite elongation. Neurons developed significantly longer

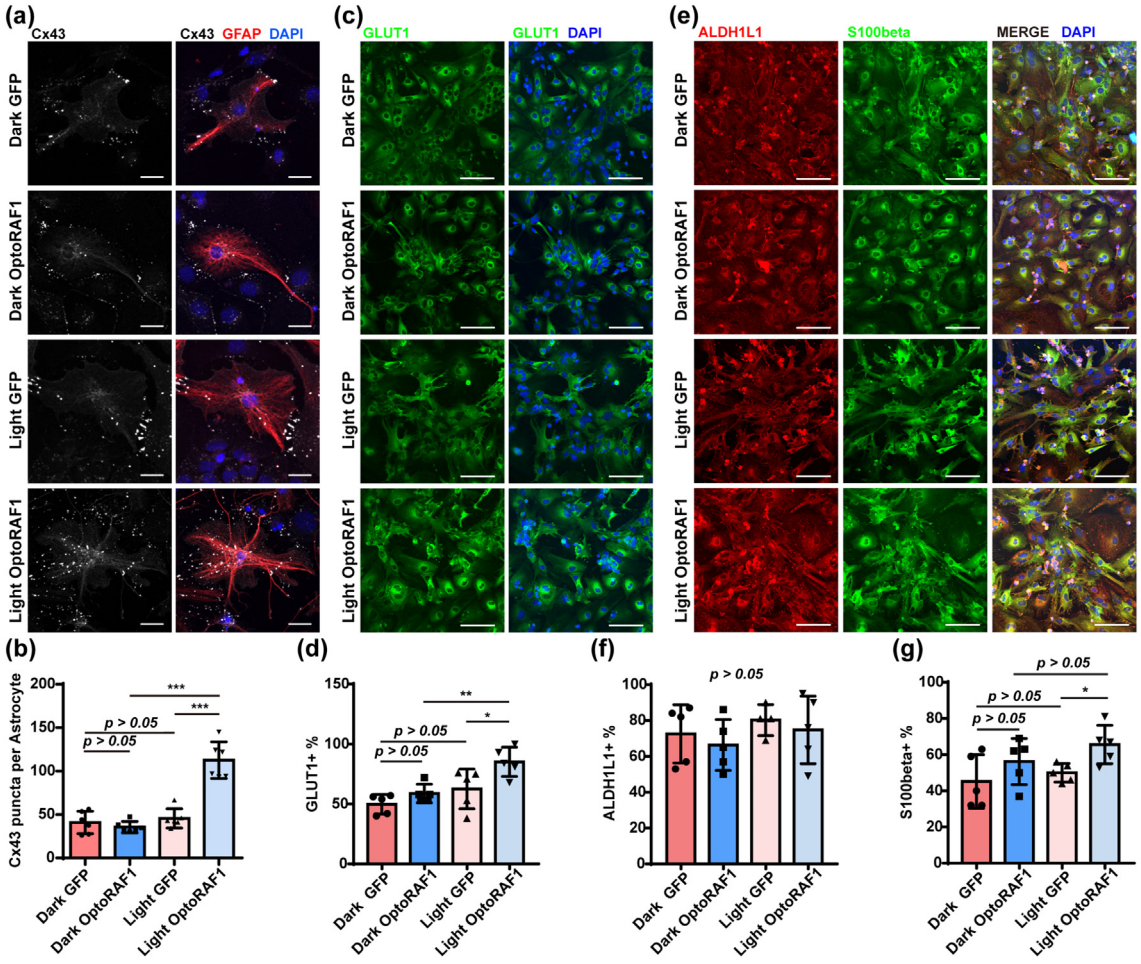

Figure 2. Light-induced OptoRAF1 activation promoted astrocyte markers expression. (a) Immunostaining of GFAP and Cx43. The scale bar represents 10 μm. (b) Quantification of Cx43 in GFAP + astrocytes (N = 3, n ≥ 10). (c) Immunostaining of GLUT1. The scale bar represents 100 μm. (d) Quantification of GLUT1 + cell percentage (N = 2, n ≥ 2). (e) Immunostaining of ALDH1L1 and S100beta. The scale bar represents 100 μm. (f) Quantification of ALDH1L1 + cell percentage (N = 2, n ≥ 2). (g) Quantification of S100beta + cell percentage (N = 2, n ≥ 2). *** $p < 0.005$, ** $p < 0.01$, * $p < 0.05$.

MAP2 + neurites in the Light-OptoRAF1 group, as compared to controls (Figure S4C). Consistently, staining of Tuj1, another neuron-specific marker, confirmed that OptoRAF1 activation did not lead to a significant change in the proportion of neurons, but resulted in longer neurites (Figure S4D ~ F).

Discussion

In this work, we applied optogenetic tools to dissect the role of RAF1 activation during astrocytogenesis. OptoRAF1 activation in neural progenitors is able to promote not only astrocytogenesis but also astrocyte maturation, which is likely to be dose dependent. However, delayed OptoRAF1 activation has little effect on the astrocyte proliferation or on astrocyte marker expression, suggesting that there could be a limited temporal window that requires RAF1 activation during astrocytogenesis. In addition, activation of OptoRAF1 does not affect neurogenesis but instead promotes neurite elongation.

The effect of RAS/RAF/MEK/ERK during astrocytogenesis is controversial. Some reports suggest that the MEK–ERK pathway represses astrocytogenesis by methylation of astrocytic genes [11,29]. On the other hand, it has been shown that MEK1/2 is both necessary and sufficient for astrocytogenesis [13]. Our data are in agreement with the latter report, as we show that RAF activation in the early stage of neural progenitor differentiation leads to increased astrocyte differentiation as well as increased expression of astrocyte-enriched genes. Furthermore, our results suggest that the functional outcome of RAF/MEK/ERK activation is time-dependent. Indeed, delayed activation of OptoRAF1 does not

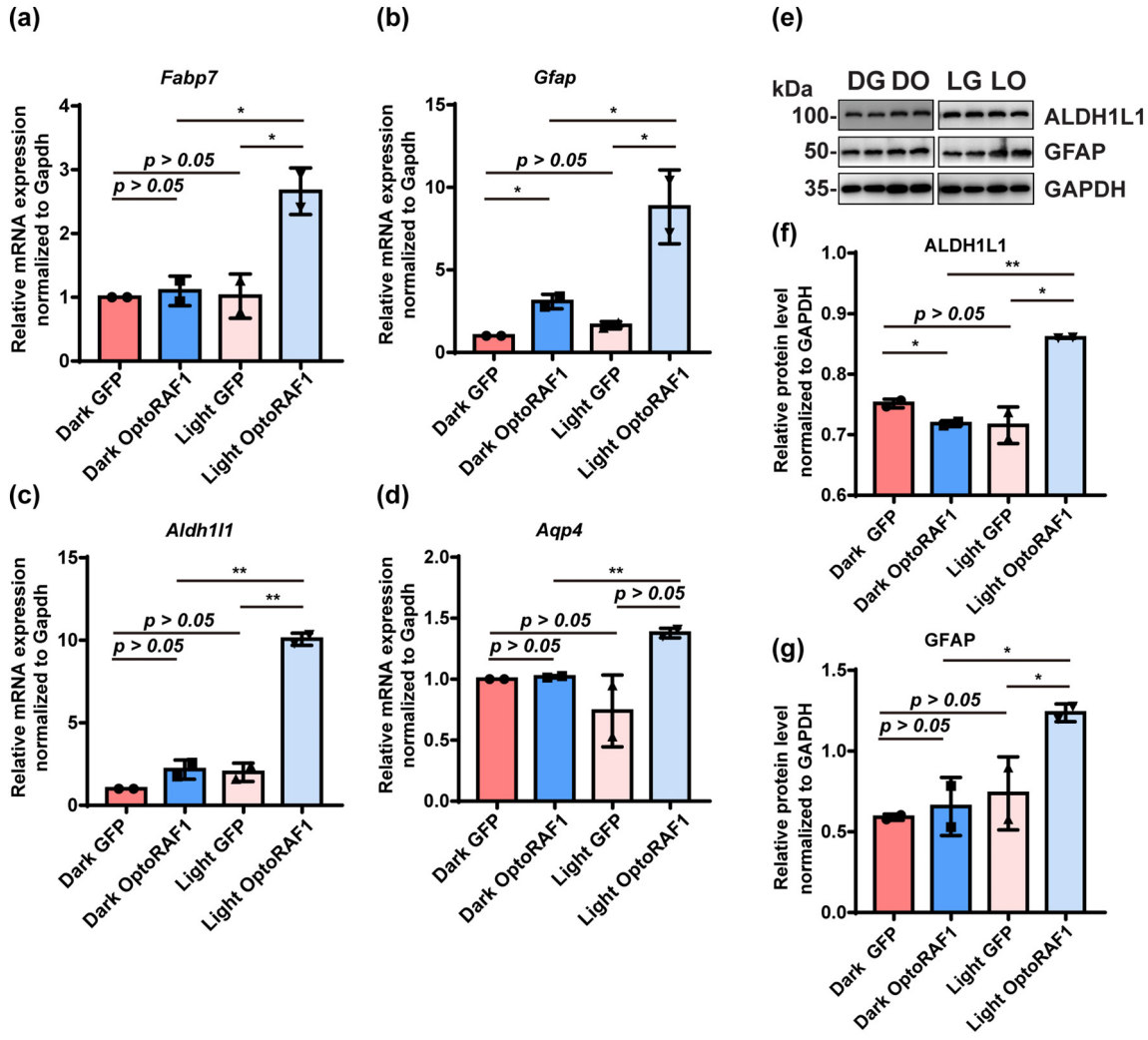

Figure 3. RT-qPCR and Western blotting confirm that light-induced OptoRAF1 activation promotes astrocyte marker gene expression. (a–d) RT-qPCR of astrocytic marker genes. (e–g) Western blot of ALDH1L1 and GFAP. ** $p < 0.01$, * $p < 0.05$.

promote astrocytogenesis. We also observed that the percentage of neurons was not altered by OptoRAF1 activation. In addition, RAF1 activation has a dose-dependent effect on astrocytogenesis.

Compared with pharmacological or gain-of-function genetic manipulation, we believe the OptoRAF1 system has several advantages. Administration of pharmacological reagents such as growth factors often leads to the activation of multiple downstream pathways, which could confound the effect of the RAF/MEK/ERK cascade. Gain-of-function overexpression of RAF mutants could bias a specific pathway, given that RAFs are multifunctional proteins. For instance, expression of $Braf^{V600E}$ resulted in the increased seizure and neuroendocrine tumor incidents, while expression of $Raf1^{L613V}$ led to enhanced memory and learning ability in mice [6,7].

The OptoRAF1 system overcomes these drawbacks through temporal induction and activation of RAF1 protein. In addition, such optogenetic system can be utilized to analyze the "dose-dependent" effect of RAF activation [30], as well as to reversibly activate the RAF proteins [25]. One significant benefit of optogenetic stimulation is in its ability for tunable temporal control; the OptoRAF1 system can be used to mimic the activation pattern of RAS–ERK pathway *in vivo*, as RAS and ERK activation under FGF treatment is oscillatory with a 2-h period [31]. Optogenetic tools have already promising applications in *in vivo* studies of embryonic development of *Xenopus* and *Drosophila* [25,32]. However, technical improvements will need to be made before being applied to study mammalian embryonic development.

In summary, we found that RAF1 activation promotes astrocytogenesis in a time-dependent manner. Our ongoing work continues to study the mechanism by which RAF1 activation regulates astrocyte gene expression. The OptoRAF1 system

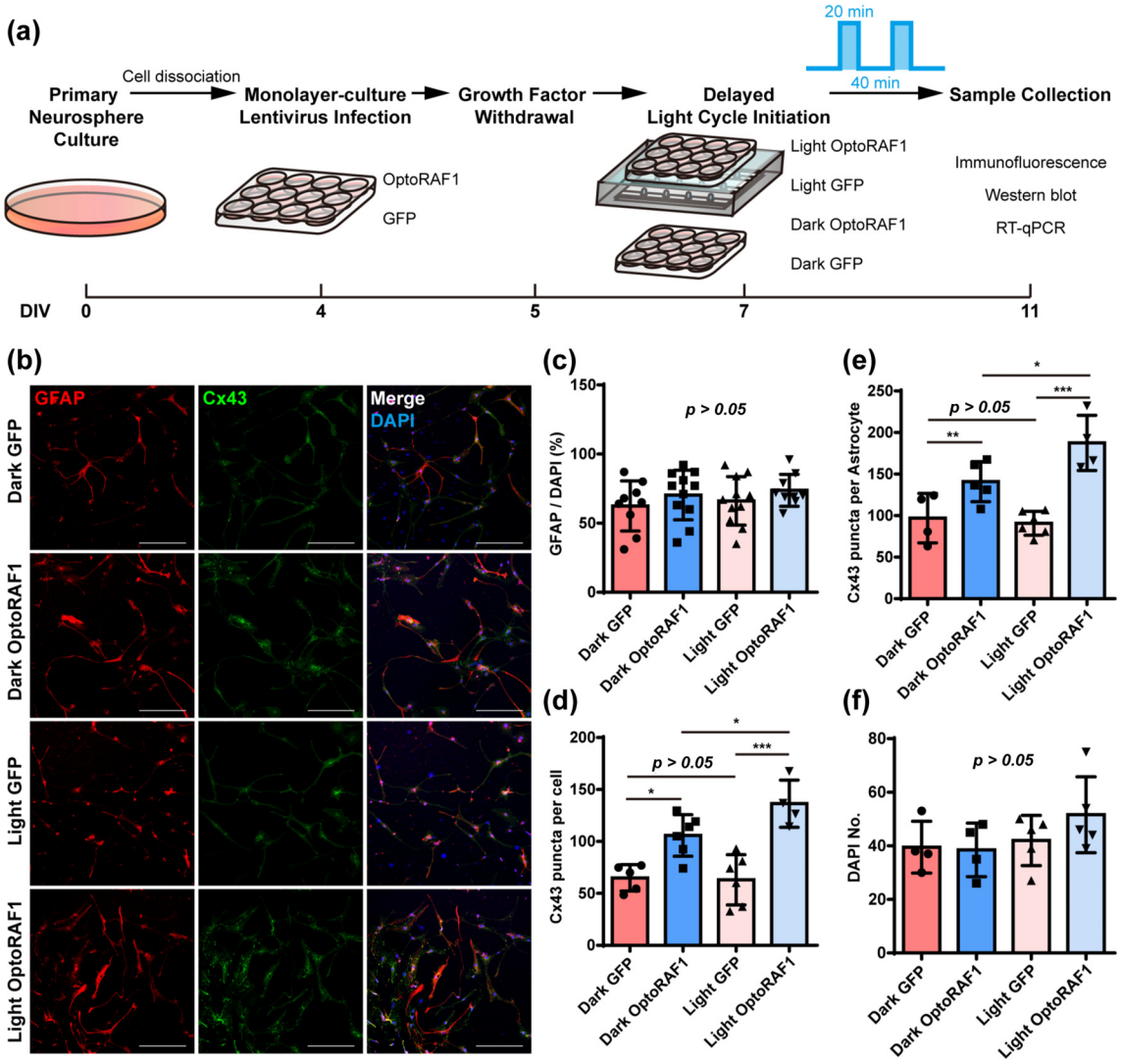

Figure 4. Delayed activation of OptoRAF1 did not promote GFAP+ astrocyte generation but promoted Cx43 expression. (a) OptoRAF1 infected neural progenitors were allowed to differentiate for 2 days, then subjected to LED illumination for 4 days before sample collection. (b) Immunostaining of GFAP and Cx43. The scale bar represents 50 μm. (c) Quantification of GFAP+ cell percentage (N = 3, n ≥ 3). (d) Quantification of Cx43 puncta normalized to GFAP+ cell count. (N = 2, n ≥ 2). (e) Quantification of Cx43 puncta per total cell count. (f) Quantification of cell number. (N = 2, n ≥ 2). *** $p < 0.005$, ** $p < 0.01$, * $p < 0.05$.

is a powerful tool to study RAF1 function by allowing flexible regulation of RAF1 activity, which can be further applied to future *in vivo* studies. This approach can also be generalized to examine the functional mechanism of other RAF proteins.

Methods and Materials

Animal

Wild-type C57BL/6J mice were euthanized by CO_2 overdose before dissection and embryo collection. All animals used in the study were maintained in a specific-pathogen-free animal facility. All procedures were performed under the approval of the Sun Yat-Sen University Institutional Animal Care and Use Committee.

Cell culture

Primary neural progenitors were isolated from embryonic day 15 mouse embryos and were cultured as neurospheres in serum-free medium (Dulbecco's modified Eagle medium/Nutrient Mixture F-12) (Gibco) with B27 supplement (Thermo), epidermal growth factor (EGF) and fibroblast growth factor (FGF) (Sigma). After culturing for 4 days, neurospheres were dissociated and seeded onto poly-D-lysine and

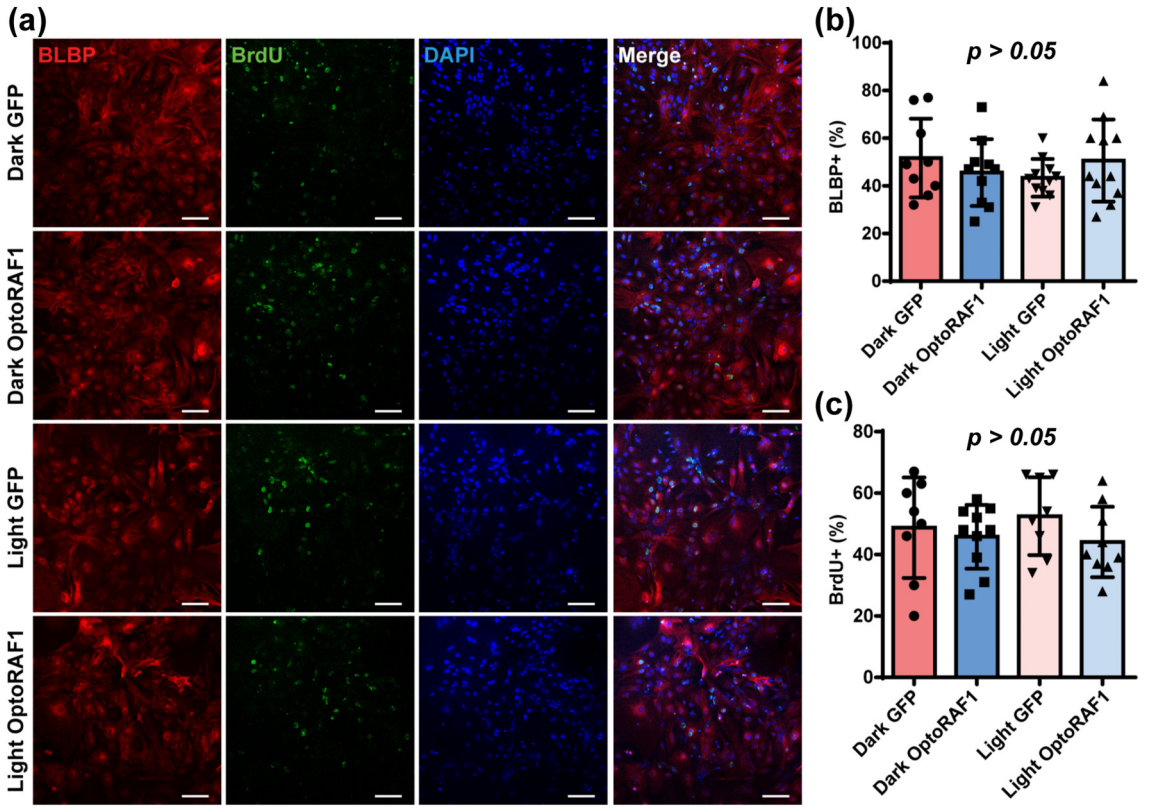

Figure 5. Delayed activation of OptoRAF1 did not promote cell proliferation. (a) Immunostaining of BLBP and BrdU after BrdU incorporation. The scale bar represents 100 μm. (b) Quantification of BLBP+ cell percentage. (c) Quantification of BrdU+ cell percentage. (N = 3, n ≥ 3).

laminin (Sigma-Aldrich) coated coverslips placed in a 12-well plate at the density of 1×10^5 cells/ml in serum-free medium with EGF/FGF (Sigma-Aldrich) supplement. EGF and FGF were withdrawn 24 h after plating. Half of the medium was changed every other day. 293T cells were maintained in Dulbecco's modified Eagle medium (Gibco) supplemented with 10% FBS (Thermo).

Plasmid construction

The OptoRAF1 plasmid was constructed as previously described [23]. The CRY-mCherry-RAF1 and CIBN-GFP-CAAX fragments were cloned to the pLJM1-eGFP vector and substituted the eGFP fragment using seamless cloning enzymes (Abclonal).

Transfection

Cells were transfected using Lipofectamine 3000 (Thermo Fisher Scientific) as per the manufacturer's protocol. Briefly, 2.0 μg of plasmid DNA was used for each well of a 6-well plate. DNA was mixed with 7.5 μl of P3000 reagent and 5 μl Lipofectamine 3000 in OptiMEM (Thermo Fisher Scientific), incubated for 5 min and added to the cells.

Lentivirus preparation and neural progenitor infection

The lentivirus was produced using third-generation lentiviral generation systems. The virus envelope plasmid and the packaging plasmids, as well as the pLJM1-eGFP/pLJM1-RAF1-CRY/pLJM1-CIBN-eGFP-CAAX plasmids, were transfected into 293T cell lines. Six hours after transfection, media were refreshed. The lentivirus-containing media was collected after 24 h and subjected to concentration by centrifugation in 100-kDa cutoff ultracentrifuge tube (Amicon) at 1500***g*** for 20 min. The lentivirus particles were then resuspended in SFM, measured for titer and stored at −80°C before used. To infect the neural progenitors, the primary neural progenitors were dissociated from neurospheres after 4 days in culture and were then plated in the lentivirus-containing serum-free medium.

Light stimulation

The LED box was constructed by plugging 12 blue LED lights in to a breadboard contained in a 12” × 7” × 3” Aluminum box covered with a translucent plastic board. The LED lights were aligned with the center of

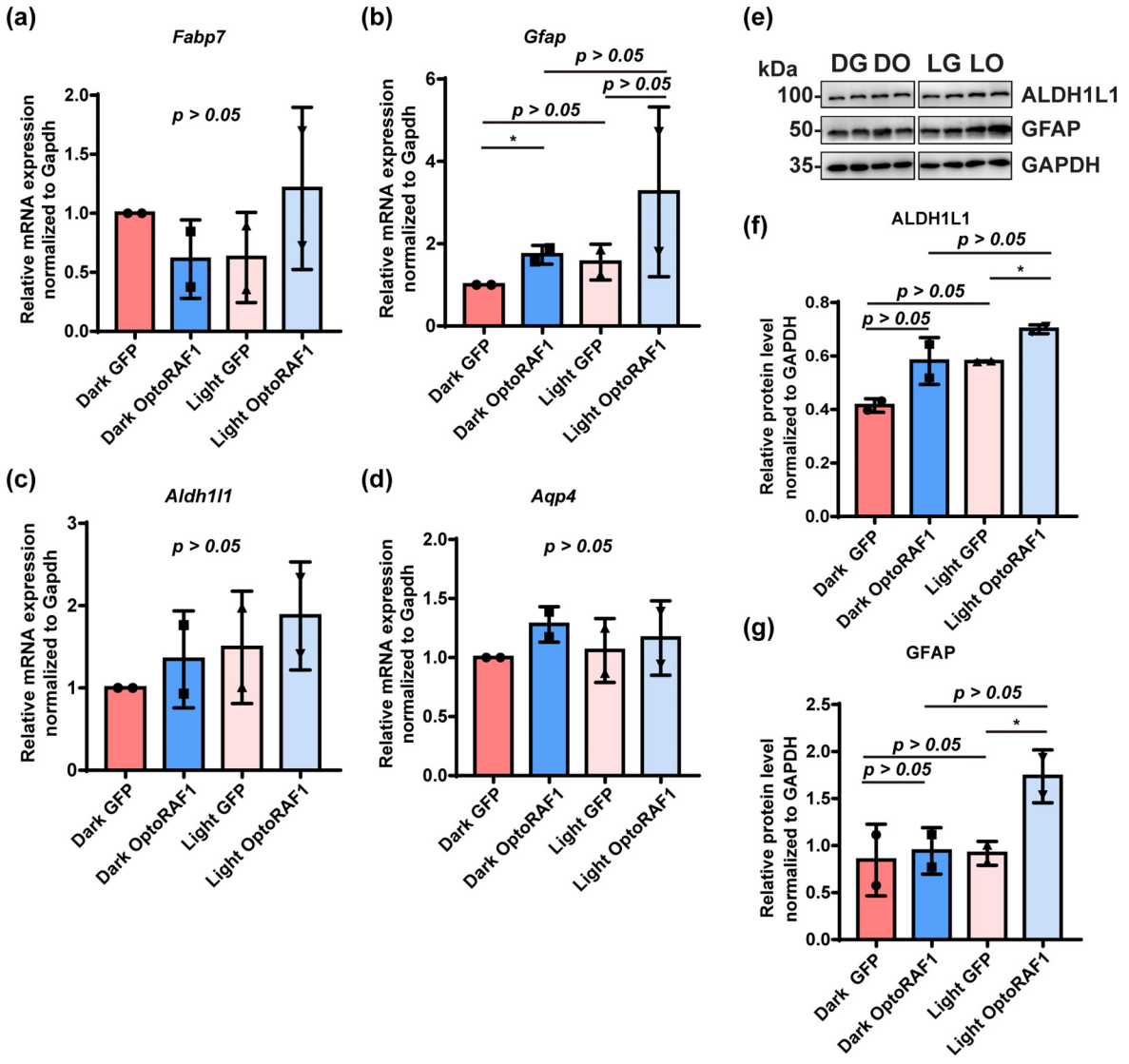

Figure 6. RT-qPCR and Western blot show that delayed activation of OptoRAF1 failed to promote astrocyte marker gene expression. (a–d) qPCR of astrocyte marker genes. (e–g) Western blot of ALDH1L1 and GFAP. * $p < 0.05$

each well of the 12-well plate and were wired with resistors. For light stimulation, cells cultured in the 12-well plate was placed on the LED box. The direct current input was set to a 20 min on/40 min off cycle [23], and the light intensity was adjusted to 25 lux at the level of the cells by adjusting the voltage.

Flow cytometry analysis

Infected neural progenitors were subjected to 15-min blue light illumination 2 days after infection. Cells were then dissociated using Accutase, fixed with 2% PFA for 30 min at room temperature and collected by centrifugation at 750***g*** for 5 min. Subsequently, cells were washed once with ice-cold PBS, incubated with pre-cooled methanol for 10 min at – 20 °C to increase cell permeability, then washed once more with PBS. After that, cells were incubated with Intracellular staining buffer (biolegend) for 30 min at room temperature for blocking, before staining with Alexa Fluor 647 anti-p-ERK1/2 antibody (biolegend) for 1 h at room temperature. Cells were then washed twice with Intracellular staining buffer and subjected to flow cytometry analysis using CytoFLEX LX (Beckman). Data were processed using the Flowjo software.

RNA-extraction and RT-qPCR

Neural progenitors were lysed directly by RNAzol (Sigma-Aldrich) and total RNA was isolated according to the manufacturer's protocol. Reverse transcription was carried out with the M-MLV Reverse Transcriptase kit from AQ according to the manufacturer's protocol. qPCR experiments were carried

out using the SYBR green qPCR kit from KAPA on an Applied Biosystems 7500 Real PCR System. qPCR primers used in the experiment can be found in Table 1. Samples were assayed in duplicate and normalized to endogenous *Gapdh*.

Protein extraction and Western blotting

Cells were lysed in RIPA buffer from Epizyme supplemented with PMSF (Sigma) on ice for 10 min, followed by 12,000***g*** centrifugation for 10 min to remove insoluble fractions. Protein concentration of the samples was measured using the BCA kit from Epizyme. Samples were then diluted, boiled in SDS sample buffer at 95 °C for 10 min and loaded into each well for SDS-PAGE. Samples were then transferred to PVDF membrane (Thermo) and immunoblotted using anti-GAPDH (BBI), anti-GFAP (Millipore) and anti-ALDH1L1 (Abcam), all diluted in 5% BSA: TBST at 1:1000, followed by appropriate HRP-conjugated secondary antibodies (Thermo) incubation (diluted in 5% non-fat milk:TBST at 1:10,000), and developed using the SuperSignal™ West Femto Maximum Sensitivity Substrate (Thermo).

Immunofluorescence

Differentiated neural progenitors on poly-D-lysine-coated coverslips were fixed with 4% paraformaldehyde for 15 min and were then permeabilized by ice-cold methanol for 5 min, followed by a PBS rinse for 10 min. The cells were then blocked with 0.2% Gelatin in PBS with 0.25% TritonX-100 for 1 h, followed by primary antibody (rabbit-anti-Cx43 (Millipore), mouse-anti-GFAP (Millipore) and rabbit-anti-BLBP (Thermo), rabbit-anti-GLUT1 (Biogen), rabbit-anti-S100beta (Abcam), rabbit-anti-ALDH1L1 (Abcam), all diluted at 1:200 in the blocking buffer) incubation at 4 °C overnight. Then, the cells were incubated in appropriate secondary antibodies (donkey-anti-mouse-AF594 (Thermo), donkey-anti-rabbit-AF-647 (Thermo), both diluted at 1:200 in the blocking buffer) for 1 h at room temperature. After washing three times in TBST, the cells on the coverslip were mounted using Prolong Gold with DAPI (Thermo) and subjected to confocal microscopy observation. The image analysis was performed with Fiji software.

Table 1. qPCR primer sequences

Name	Sequence
mGapdh_rtq_F	CCCCAGCAAGGACACTGAGCAA
mGapdh_rtq_R	GTGGGTGCAGCGAACTTTATTGATG
mGfap_rtq_F	AACTGAACCAGCTTCGAGCC
mGfap_rtq_R	CCGAGGTCCTGTGCAAAGTT
mAldh1l1_rtq_F	TGGGCAGAAGCTGACGTTTT
mAldh1l1_rtq_R	GATGAGTCCCGCTTTGGTGA
mAqp4_rtq_F	CTCACGGCTCTGCCAGTAAA
mAqp4_rtq_R	TTGGTGTCATCCACAAGGCA
mFabp7_rtq_F	TGATCCGGACACAATGCACA
mFabp7_rtq_R	AGCTTGTCTCCATCCAACCG

Statistic

Statistical significance was determined by Student's *t*-test using GraphPad Prism 6.01. A p value < 0.05 was considered significant. Unless otherwise specified, data were presented as mean and the standard deviation (mean ± SD).

Supplementary data to this article can be found online at https://doi.org/10.1016/j.jmb.2020.06.020.

CRediT authorship contribution statement

Yixun Su: Conceptualization, Methodology, Visualization, Investigation, Writing - original draft. **Xiaomin Huang:** Visualization, Investigation. **Zhangsen Huang:** Investigation.**Taida Huang:**Validation. **Tao Li:** Validation.**Huaxun Fan:** Methodology. **Kai Zhang:** Supervision, Methodology. **Chenju Yi:** Supervision, Writing - review & editing.

Acknowledgments

This work was supported by grants from the National Nature Science Foundation of China (NSFC 81971309) and Guangdong Basic and Applied Basic Research Foundation (2019A1515011333) and the Fundamental Research Funds for the Central Universities (F7201931620002). This research was also supported by the School of Molecular Cell Biology at the University of Illinois at Urbana–Champaign (K.Z.).

Received 22 March 2020;
Received in revised form 18 June 2020;
Accepted 19 June 2020
Available online 26 June 2020

Keywords:
RAF1;
Optogenetic;
OptoRAF1;
neural progenitor;
astrocytogenesis

†Y.S. and X.H. contributed equally to this work.

Abbreviations used:
GLUT1, glucose transporter 1; ALDH1L1, Aldehyde Dehydrogenase 1 Family Member L1; EGF, epidermal growth factor; FGF, fibroblast growth factor.

References

[1] Namihira, M., Nakashima, K., (2013). Mechanisms of astrocytogenesis in the mammalian brain. *Curr. Opin. Neurobiol.*, **23**, 921–927.

[2] Qian, X., Shen, Q., Goderie, S.K., He, W., Capela, A., Davis, A.A., et al., (2000). Timing of CNS cell generation: a programmed sequence of neuron and glial cell production from isolated murine cortical stem cells. *Neuron.*, **28**, 69–80.

[3] Lavoie, H., Therrien, M., (2015). Regulation of RAF protein kinases in ERK signalling. *Nat. Rev. Mol. Cell. Biol.*, **16**, 281–298.

[4] Rhee, Y.H., Yi, S.H., Kim, J.Y., Chang, M.Y., Jo, A.Y., Kim, J., et al., (2016). Neural stem cells secrete factors facilitating brain regeneration upon constitutive Raf–Erk activation. *Sci. Rep.*, **6**, 32025.

[5] Tien, A.C., Tsai, H.H., Molofsky, A.V., McMahon, M., Foo, L.C., Kaul, A., et al., (2012). Regulated temporal–spatial astrocyte precursor cell proliferation involves BRAF signalling in mammalian spinal cord. *Development*, **139**, 2477–2487.

[6] Urosevic, J., Sauzeau, V., Soto-Montenegro, M.L., Reig, S., Desco, M., Wright, E.M., et al., (2011). Constitutive activation of B-Raf in the mouse germ line provides a model for human cardio-facio-cutaneous syndrome. *Proc. Natl. Acad. Sci. U. S. A.*, **108**, 5015–5020.

[7] Holter, M.C., Hewitt, L.T., Koebele, S.V., Judd, J.M., Xing, L., Bimonte-Nelson, H.A., et al., (2019). The Noonan Syndrome-linked Raf1L613V mutation drives increased glial number in the mouse cortex and enhanced learning. *PLoS Genet.*, **15**, e1008108.

[8] Magarinos, M., Aburto, M.R., Sanchez-Calderon, H., Munoz-Agudo, C., Rapp, U.R., Varela-Nieto, I., (2010). RAF kinase activity regulates neuroepithelial cell proliferation and neuronal progenitor cell differentiation during early inner ear development. *PLoS One.*, **5**, e14435.

[9] Kolkova, K., Novitskaya, V., Pedersen, N., Berezin, V., Bock, E., (2000). Neural cell adhesion molecule-stimulated neurite outgrowth depends on activation of protein kinase C and the Ras-mitogen-activated protein kinase pathway. *J. Neurosci.*, **20**, 2238–2246.

[10] Menard, C., Hein, P., Paquin, A., Savelson, A., Yang, X.M., Lederfein, D., et al., (2002). An essential role for a MEK-C/EBP pathway during growth factor-regulated cortical neurogenesis. *Neuron.*, **36**, 597–610.

[11] Paquin, A., Barnabe-Heider, F., Kageyama, R., Miller, F.D., (2005). CCAAT/enhancer-binding protein phosphorylation biases cortical precursors to generate neurons rather than astrocytes in vivo. *J. Neurosci.*, **25**, 10747–10758.

[12] Kong, S.Y., Kim, W., Lee, H.R., Kim, H.J., (2018). The histone demethylase KDM5A is required for the repression of astrocytogenesis and regulated by the translational machinery in neural progenitor cells. *FASEB J.*, **32**, 1108–1119.

[13] Li, X., Newbern, J.M., Wu, Y., Morgan-Smith, M., Zhong, J., Charron, J., et al., (2012). MEK is a key regulator of gliogenesis in the developing brain. *Neuron.*, **75**, 1035–1050.

[14] Khamo, J.S., Krishnamurthy, V.V., Sharum, S.R., Mondal, P., Zhang, K., (2017). Applications of optobiology in intact cells and multicellular organisms. *J. Mol. Biol.*, **429**, 2999–3017.

[15] Zhang, K., Cui, B., (2015). Optogenetic control of intracellular signaling pathways. *Trends Biotechnol.*, **33**, 92–100.

[16] Guglielmi, G., Falk, H.J., De Renzis, S., (2016). Optogenetic control of protein function: from intracellular processes to tissue morphogenesis. *Trends Cell Biol.*, **26**, 864–874.

[17] Tischer, D., Weiner, O.D., (2014). Illuminating cell signalling with optogenetic tools. *Nat. Rev. Mol. Cell. Biol.*, **15**, 551–558.

[18] Shin, Y., Berry, J., Pannucci, N., Haataja, M.P., Toettcher, J.E., Brangwynne, C.P., (2017). Spatiotemporal control of intracellular phase transitions using light-activated optodroplets. *Cell.*, **168**, 159–171 e14.

[19] Johnson, H.E., Goyal, Y., Pannucci, N.L., Schupbach, T., Shvartsman, S.Y., Toettcher, J.E., (2017). The spatiotemporal limits of developmental Erk signaling. *Dev. Cell.*, **40**, 185–192.

[20] Tichy, A.M., Gerrard, E.J., Legrand, J.M.D., Hobbs, R.M., Janovjak, H., (2019). Engineering strategy and vector library for the rapid generation of modular light-controlled protein–protein interactions. *J. Mol. Biol.*, **431**, 3046–3055.

[21] Redchuk, T.A., Karasev, M.M., Verkhusha, P.V., Donnelly, S.K., Hulsemann, M., Virtanen, J., et al., (2020). Optogenetic regulation of endogenous proteins. *Nat. Commun.*, **11**, 605.

[22] Yu, D., Lee, H., Hong, J., Jung, H., Jo, Y., Oh, B.H., et al., (2019). Optogenetic activation of intracellular antibodies for direct modulation of endogenous proteins. *Nat. Methods.*, **16**, 1095–1100.

[23] Zhang, K., Duan, L., Ong, Q., Lin, Z., Varman, P.M., Sung, K., et al., (2014). Light-mediated kinetic control reveals the temporal effect of the Raf/MEK/ERK pathway in PC12 cell neurite outgrowth. *PLoS One.*, **9**, e92917.

[24] Ong, Q., Guo, S., Duan, L., Zhang, K., Collier, E.A., Cui, B., (2016). The timing of Raf/ERK and AKT activation in protecting PC12 cells against oxidative stress. *PLoS One.*, **11**, e0153487.

[25] Krishnamurthy, V.V., Khamo, J.S., Mei, W., Turgeon, A.J., Ashraf, H.M., Mondal, P., et al., (2016). Reversible optogenetic control of kinase activity during differentiation and embryonic development. *Development*, **143**, 4085–4094.

[26] Wilson, M.Z., Ravindran, P.T., Lim, W.A., Toettcher, J.E., (2017). Tracing information flow from Erk to target gene induction reveals mechanisms of dynamic and combinatorial control. *Mol. Cell.*, **67**, 757–769 e5.

[27] Cao, F.J., Zhang, X., Liu, T., Li, X.W., Malik, M., Feng, S.Q., (2013). Up-regulation of Ras/Raf/ERK1/2 signaling in the spinal cord impairs neural cell migration, neurogenesis, synapse formation, and dendritic spine development. *Chin. Med. J.*, **126**, 3879–3885.

[28] Lee, H.R., Lee, J., Kim, H.J., (2019). Differential effects of MEK inhibitors on rat neural stem cell differentiation: repressive roles of MEK2 in neurogenesis and induction of astrocytogenesis by PD98059. *Pharmacol. Res.*, **149**, 104466.

[29] Miller, F.D., Gauthier, A.S., (2007). Timing is everything: making neurons versus glia in the developing cortex. *Neuron.*, **54**, 357–369.

[30] Bugaj, L.J., Sabnis, A.J., Mitchell, A., Garbarino, J.E., Toettcher, J.E., Bivona, T.G., et al., (2018). Cancer mutations and targeted drugs can disrupt dynamic signal encoding by the Ras–Erk pathway. *Science*, **361.**

[31] Nakayama, K., Satoh, T., Igari, A., Kageyama, R., Nishida, E., (2008). FGF induces oscillations of Hes1 expression and Ras/ERK activation. *Curr. Biol.*, **18**, R332–R334.

[32] Johnson, H.E., Shvartsman, S.Y., Toettcher, J.E., (2019). Optogenetic rescue of a developmental pattern2019.